

## Significance of a local temperature rise in nanoindentation testing

A. C. FISCHER-CRIPPS

CSIRO Division of Telecommunications and Industrial Physics, PO Box 218 Lindfield, NSW 2070, Australia  
E-mail: tony.cripps@csiro.au

Depth-sensing indentation, on the sub-micron scale—nanoindentation, is now routinely used as a means of measurement of the mechanical properties of thin films and small volumes of materials. Significant effort has been applied to an understanding of the load displacement response in order to obtain meaningful data for elastic modulus and hardness with respect to corrections for instrument and materials related issues [1]. The most common indenter used in nanoindentation experiments is the three-sided pyramidal Berkovich indenter with which it is usually desired to obtain a fully-developed plastic zone in the specimen material corresponding to indenter displacements of less than a micron. The formation of the plastic zone is physically associated with the generation of heat within the specimen material, and as a consequence, a temperature rise. Such a temperature rise results in the thermal expansion of the specimen material in the vicinity of the indenter, and this may in turn be registered in the displacement readings taken during the indentation—thus having an undesirable effect on the subsequent analysis of the load-displacement data. Such an effect has hitherto not been considered in the analysis of depth-sensing nanoindentation test data. The purpose of the present work is to present a first-order treatment of the phenomenon, and to stimulate further study of the related material issues.

Although most analyses of nanoindentation test data assume a quasi-static process, typical indentations are usually accomplished over a matter of a few seconds, and for the purpose of the present discussion, we shall assume that the process is adiabatic. The net work of indentation will be assumed to be accounted for by heat within the plastic zone, and any dissipative effects due to friction at the interface between the indenter and specimen will be ignored.

The work of indentation  $U_p$  can be easily calculated by numerically calculating the net area under the load-displacement curve. The volume  $V_p$  of material affected by plastic deformation can be calculated from the dimensions of the plastic zone, which in turn are more easily determined by finite element analysis. The mass of material thus affected is calculated from the density  $\rho$  and volume  $V$  of the plastic zone. The resulting average temperature rise  $\Delta T$  is thus given by:

$$\Delta T = \frac{U_p}{\rho V c} \quad (1)$$

where  $c$  is the specific heat of the specimen material. Assuming that the size of the plastic zone  $l$  is a mea-

sure of the dimension of the material undergoing “expansion,” the change in linear dimension  $\Delta l$  resulting from the average temperature rise given in Equation 1 is thus:

$$\Delta l = l \alpha \Delta T \quad (2)$$

where  $\alpha$  is the thermal expansion coefficient.

Two representative materials, fused silica and aluminum, were selected for the study. In both cases, experiments were performed using a conventional nanoindenter [2] with a Berkovich indenter to obtain representative load-displacement curves. These curves were used to validate the response of the same test replicated using an axis-symmetric, elastic-plastic finite element analysis in which the Berkovich indenter was treated in terms of a cone of semi-angle  $70.3^\circ$ . Values of elastic modulus and hardness (factored down by a constraint factor) were used in the finite element modelling along with a simple elastic-perfectly plastic stress-strain behavior in conjunction with the Tresca criterion for plastic flow. Fig. 1 shows the load-displacement curves obtained. For the experimental data in Fig. 1, no indenter shape correction was applied. Values for  $U_p$  and  $V_p$  were obtained from the load-displacement curves and the extent of the maximum shear stress contour from the finite element model for each material for two loads, 50 and 1 mN. It is important to note that the volume of plastic  $V_p$  zone in each case was determined from the cross-sectional calculated area of the plastic zone. Table I summarizes the results obtained. Fig. 2 shows the dimensions of the relevant quantities where the sizes of the plastic zones are drawn to scale for both materials.

It is interesting to note that the temperature rise in the different materials depends very much on the volume of the plastic zone. In fused silica, where the volume of plastically deformed material is much less compared to that in the case of aluminum, the temperature within the plastic zone is correspondingly much higher despite the greater degree of elastic recovery in the former. It is also of interest to observe that the predicted average temperature of material appears to be independent of the load. This is a consequence of the geometrical similarity of the contact. For a given temperature rise, Equation 1 shows that the plastic energy  $U_p$  must scale directly with the volume of the plastic zone, the other terms being constant. For a given increment of indenter displacement, we have:

$$U = P \delta h = \frac{P}{A} \delta V \quad (3)$$

TABLE I Results obtained by finite element analysis of load-displacement curve for fused silica and aluminum for an indentation with a conical indenter of half-angle  $70.3^\circ$  with elastic-plastic analysis with Tresca criterion for plastic flow. Column headings show the material properties used in the finite element, modelling, and calculations

	Fused silica ( $E = 72.5$ GPa, $\nu = 0.17$ , $Y = 6.6$ GPa, $\rho = 2200$ kgm $^{-3}$ , $c = 740$ Jkg $^{-1}$ °C $^{-1}$ , $\alpha = 5.5 \times 10^{-7}$ °C $^{-1}$ )		Aluminum ( $E = 70$ GPa, $\nu = 0.34$ , Y 530 = GPa, $\rho = 2700$ kgm $^{-3}$ , $c = 900$ Jkg $^{-1}$ °C $^{-1}$ , $\alpha = 2.35 \times 10^{-5}$ °C $^{-1}$ )	
	1 mN	50 mN	1 mN	50 mN
Maximum penetration depth $h_t$ (nm)	95.4	670	159.7	1102
Average dimension of plastic zone $l$ (m)	$3.33 \times 10^{-7}$	$1.20 \times 10^{-6}$	$1.38 \times 10^{-6}$	$1.0 \times 10^{-5}$
Volume of plastic zone $V_p$ (m $^3$ )	$4.54 \times 10^{-20}$	$1.42 \times 10^{-17}$	$5.50 \times 10^{-18}$	$2.09 \times 10^{-15}$
Work of indentation $U_p$ (J)	$7.4 \times 10^{-12}$	$2.60 \times 10^{-9}$	$4.43 \times 10^{-11}$	$1.5 \times 10^{-8}$
Mass $m$ (kg)	$9.96 \times 10^{-17}$	$3.13 \times 10^{-14}$	$1.49 \times 10^{-14}$	$5.65 \times 10^{-12}$
Temperature rise $\Delta T$ (°C)	100.4	112.0	3.3	2.9
Change in linear dimension $\Delta l$ (nm)	0.019	0.137	0.107	0.69
Volume of residual impression $V_r$ (m $^3$ )	$5.37 \times 10^{-22}$	$1.96 \times 10^{-19}$	$2.39 \times 10^{-20}$	$7.90 \times 10^{-18}$
Ratio of $V_p/V_r$	84.6	72.5	230	265
Apparent hardness $U_p/V_r$ (GPa)	13.8	13.24	1.85	1.9

where if  $\delta V$  is given as the volume of the residual impression, then  $U$  is  $U_p$  and the quantity  $P/A$  is equivalent to the apparent hardness [3]. Thus, for a geometrically similar indentation, such as that made with a cone

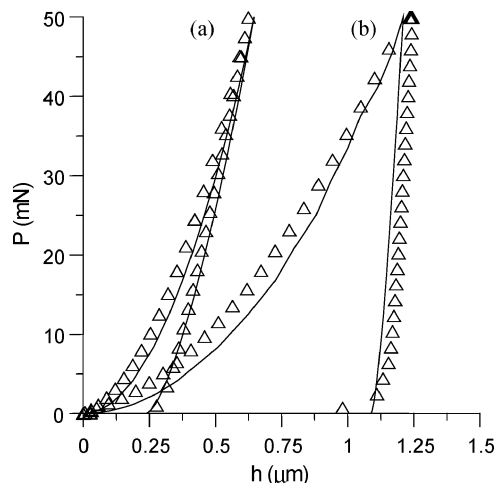


Figure 1 Load-displacement curves for (a) fused silica, and (b) aluminum. Symbols indicate experimental results and solid lines indicate finite element results. The area enclosed by the curves is the net work of indentation  $U_p$ .

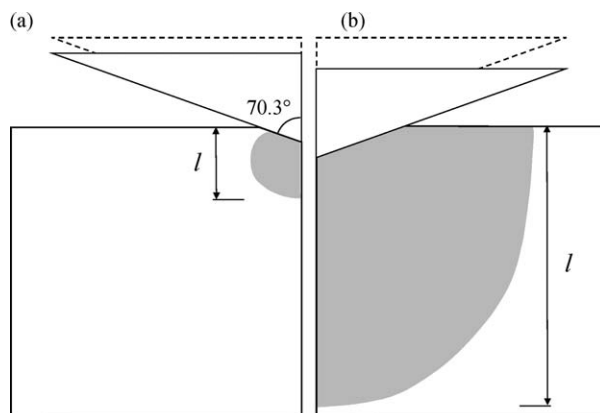


Figure 2 Schematic of plastic zone and indentation geometry for axis-symmetric finite element model for (a) fused silica, (b) aluminum. Sizes of plastic zone (shaded) are drawn to scale from elastic-plastic finite element results for the same load in each material. Only a portion of the model near the contact is shown.

or a pyramid, the volume of residual impression scales with the volume of the plastic zone, and so a constant value of temperature rise is expected independent of the load.

The results shown in Table I show that the thermal expansions ( $\Delta l$ ), despite the significant temperature increases, are only a very small fraction of the overall penetration depth and so are unlikely to have a significant deleterious effect on the analysis of nanoindentation test data. Even considering the extraordinary low coefficient of thermal expansion in the case of fused silica, thermal expansion from the plastic zone in other nominally brittle materials are unlikely to affect the results of a nanoindentation test to an appreciable extent.

In the present work, the average temperature rise was calculated using a very simple first-order analysis. Lawn *et al.* [4] present a similar analysis of experimental data for soda-lime glass and further show that the temperature distribution within the plastic zone can result in a very significant temperature rise near the contact surface, especially in very rapid contacts, leading to localised melting of the specimen. Yoshioka and Yoshioka [5] measured the temperature rise in BaF, also under impact loading, using a thermal imaging apparatus and found only a very small temperature increase, but their results may have been affected by the relatively coarse spatial resolution of the thermal sensor. Local temperature rises from plasticity in the contact region have, to the present author's knowledge, not thus far been considered in analysis methods that use the data in load-displacement curves in nanoindentation. The results presented here show that the change in dimension of the contact, resulting from plasticity induced by the indentation, is not a significant proportion of the total penetration depth in nanoindentation tests on two representative materials. The results also show that the average temperature increase is significant, and fairly independent of load in the case of a conical indenter. The resulting material issues (such as indentation size effects, local melting, changes in viscosity, creep, etc.) may well be worthy of further consideration and deeper study for a given material system.

## Acknowledgment

The author thanks B.R. Lawn for his useful discussions.

## References

1. A. C. FISCHER-CRIPPS, "Nanoindentation" (Springer-Verlag, New York, 2002).
2. UMIS<sup>®</sup>, CSIRO Division of Telecommunications and Industrial Physics, Bradfield Rd, West Lindfield, NSW 2070, Australia.

3. M. SAKAI, *Acta. Metal. Mater.* **41**(6) (1993) 1751.
4. B. R. LAWN, B. J. HOCKEY and S. M. WIEDERHORN, *J. Amer. Ceram. Soc.* **63**(5/6) (1980) 356.
5. N. YOSHIOKA and M. YOSHIOKA, *Phil. Mag. A* **74**(5) (1996) 1273.

*Received 10 February  
and accepted 30 April 2004*